

Programmable polarization-independent spectral phase compensation and pulse shaping

R. D. Nelson, D. E. Leaird, and A. M. Weiner

Purdue University, School of Electrical & Computer Engineering, 465 Northwestern Ave., West Lafayette, IN 47907-2035

rmelson@ecn.purdue.edu, leaird@ecn.purdue.edu, amw@ecn.purdue.edu

Abstract: We report the first use of a double-layer liquid crystal modulator array for spectral phase pulse shaping that operates independent of polarization. Such insensitivity to polarization is crucial for fiber applications, e.g., dispersion compensation.

©2003 Optical Society of America

OCIS codes: (060.2330) Fiber optics communications; (320.5540) Pulse shaping; (070.2580) Fourier optics

References and Links

1. A.M. Weiner, "Femtosecond Pulse Shaping Using Spatial Light Modulators," *Rev. Sci. Instr.* **71**, 1929-1960 (2000).
2. R.J. Levis, G.M. Menkir, and H. Rabitz, "Selective Bond Dissociation and Rearrangement with Optimally Tailored, Strong-Field Laser Pulses," *Science* **292**, 709-713 (2001).
3. C.-C. Chang, H.P. Sardesai, and A.M. Weiner, "Dispersion-Free Fiber Transmission for Femtosecond Pulses Using a Dispersion-Compensating Fiber and a Programmable Pulse Shaper," *Opt. Lett.* **23**, 283-285 (1998).
4. S. Shen and A.M. Weiner, "Complete Dispersion Compensation for 400-Fs Pulse Transmission over 10-Km Fiber Link Using Dispersion Compensating Fiber and Spectral Phase Equalizer," *IEEE Phot. Tech. Lett.* **11**, 827-829 (1999).
5. H. Takenouchi, T. Goh, and T. Ishii, "8 Thz Bandwidth Dispersion-Slope Compensator Module for Multiband 40 Gbit/s WDM Transmission Systems Using an AWGs and Spatial Phase Filter," *Electron. Lett.* **37**, 777-778 (2001).
6. M. Shirasaki and S. Cao, "Compensation of Chromatic Dispersion and Dispersion Slope using a Virtually Imaged Phased Array," presented at the Optical Fiber Communications Conference, Anaheim, CA, 17-22 Mar. 2001.
7. T. Sano, T. Iwashima, M. Katayama, T. Kanie, M. Harumoto, M. Shigehara, H. Suganuma, and M. Nishimura, "Novel Multi-Channel Tunable Chromatic Dispersion Compensator Based on MEMS & Diffraction Grating," presented at the Optical Fiber Communications Conference, Atlanta, GA, 23-28 Mar. 2003.
8. T. Brixner, M. Strehle, and G. Gerber, "Feedback-Controlled Optimization of Amplified Femtosecond Laser Pulses," *Appl. Phys. B* **68**, 281-284 (1999).
9. E. Zeek, R. Bartels, M. Murnane, H. Kapteyn, S. Backus, and G. Vdovin, "Adaptive pulse compression for transform-limited 15-fs high-energy pulse generation," *Opt. Lett.* **25**, 587-589 (2000).
10. A.M. Weiner, D.E. Leaird, J.S. Patel, and J.R. Wullert, "Programmable Shaping of Femtosecond Pulses by Use of a 128-Element Liquid-Crystal Phase Modulator," *IEEE J. Quantum Electron.* **28**, 908-920 (1992).
11. M.M. Wefers and K.A. Nelson, "Generation of High-Fidelity Programmable Ultrafast Optical Waveforms," *Opt. Lett.* **20**, 1047-1049 (1995).
12. J.X. Tull, M.A. Dugan, and W.S. Warren, "High Resolution, Ultrafast Laser Pulse Shaping and Its Applications," *Adv. Magn. Opt. Reson.* **20**, 1 (1997).
13. T. Brixner and G. Gerber, "Femtosecond Polarization Pulse Shaping," *Opt. Lett.* **26**, 557-559 (2001).
14. K. Tamura, H. A. Haus and E. P. Ippen, "Self-Starting Additive Pulse Mode-Locked Erbium Fibre Ring Laser," *Electron. Lett.* **28**, 2226-2228 (1992).

1. Introduction

Fourier transform pulse shapers [1] are an important tool for controlling the waveforms of ultrafast optical pulses and are now widely applied for applications ranging from coherent quantum control [2] to dispersion compensation. With respect to dispersion compensation, programmable pulse shaping has been used to demonstrate distortionless propagation of 400 fs pulses over 10 km dispersion-compensated fiber links via equalization of higher-order spectral phase [3,4]. More recently, several groups are developing pulse shaping technologies for dispersion slope compensation relevant to 40 Gb/s fiber transmission [5-7]. Programmable pulse shaping is also used with femtosecond laser systems, e.g., to compensate higher-order chirp and consequently improve pulse quality in femtosecond chirped pulse amplifiers [8,9]. In femtosecond laser applications, the input to the pulse shaper has a stable, well-characterized linear polarization. However, in fiber optic applications the input polarization is usually not known and may vary with time. Therefore, polarization-independent pulse shaping operation is highly desirable for fiber applications. In this paper for the first time to our knowledge, we report polarization-independent spectral phase pulse shaping, which we demonstrate in the context of a simple fiber dispersion compensation experiment.

Fourier transform pulse shaping is based on spatial masking of spatially dispersed optical frequency spectra [1]. Various spatial light modulators have been used, including liquid crystal modulator arrays (LCMs) [10,11], acousto-optics [12], and deformable mirrors [9]. The most widely applied of these technologies is the LCM, which provides a unique combination of large pixel count (necessary to support high pulse shaping complexity) and 100% duty factor operation (necessary for compatibility with high-repetition-rate signal sources characteristic of fiber optic communications). LCMs are available both in one-layer and two-layer configurations. In the one-layer case [10], phase control of a specific linear polarization can be achieved; however, the orthogonal polarization is not controllable. Two-layer LCMs are usually constructed with one liquid crystal layer oriented at 45° and the other oriented at -45° [11]. In normal pulse shaping operation, the retardances of the two layers are voltage-controlled on a pixel-by-pixel basis to manipulate the phase and the output polarization (converted to intensity via a polarizer) for fixed vertically or horizontally polarized input light. Spectral phase and partial spectral polarization control have also been demonstrated in a similar setup but omitting the output polarizer, leading to pulses with a time-dependent polarization state [13]. These experiments required a factor of three attenuation of one of the output polarizations to compensate for polarization dependent loss (PDL) of the grating spectral disperser. In our experiments we achieve polarization-independent spectral phase control by introducing a polarization-independent operating mode of the LCM in conjunction with a low-PDL telecommunications grating.

2. Theory

The theory behind polarization-insensitive operation is best understood by Jones calculus. The Jones matrix for any single pixel of a two-layer LCM, J_{LCM} , in a rotated coordinate frame where the coordinate axes are along $\pm 45^\circ$, can be written as follows:

$$J_{LCM} = \begin{bmatrix} \exp(j\psi_{2S}) & 0 \\ 0 & \exp(j\psi_{2L}(V_2)) \end{bmatrix} \begin{bmatrix} \exp(j\psi_{1L}(V_1)) & 0 \\ 0 & \exp(j\psi_{1S}) \end{bmatrix} \quad (1)$$

Here $\psi_{kL}(V_k)$ refers to the optical phase corresponding to propagation through the k^{th} liquid crystal layer for light polarized along the long LC axis ($k = 1:2$). Application of a voltage produces a longitudinal electric field which rotates the LC molecules toward the direction of the applied field. As a result ψ_{kL} is a function of the voltage V_k . ψ_{kS} is the phase for light

polarized along the short LC axis in the k^{th} liquid crystal layer and is independent of applied voltage. Eq. (1) can be manipulated to yield:

$$J_{LCM} = \exp\left(j \frac{\psi_{1L}(V_1) + \psi_{2L}(V_2)}{2}\right) \exp\left(j \frac{\psi_{1S} + \psi_{2S}}{2}\right) \times \begin{bmatrix} \exp\left(j \frac{\Delta_2(V_2) - \Delta_1(V_1)}{2}\right) & 0 \\ 0 & \exp\left(j \frac{\Delta_1(V_1) - \Delta_2(V_2)}{2}\right) \end{bmatrix} \quad (2)$$

where $\Delta_k(V_k) = \psi_{kS} - \psi_{kL}(V_k)$ is the voltage-dependent retardance of the k^{th} layer. The key to polarization-insensitive operation is to choose the voltage for the two layers to produce the same retardance, i.e., $\Delta_1(V_1) = \Delta_2(V_2)$. As a result of such common-mode operation, J_{LCM} reduces to:

$$\exp\left(j \frac{\psi_{1L}(V_1) + \psi_{2L}(V_2)}{2}\right) \exp\left(j \frac{\psi_{1S} + \psi_{2S}}{2}\right) \begin{bmatrix} 1 & 0 \\ 0 & 1 \end{bmatrix} \quad (3)$$

where the 1st phase factor represents a voltage variable phase, the 2nd phase factor represents a fixed phase resulting from the minimum optical thickness of the layers and the identity matrix represents a polarization transformation of unity. The voltage-dependent factor allows us to pick a phase that remains constant for arbitrary input polarization. Furthermore, the input state of polarization is preserved. Thus for an array of N pixels, we have an N -pixel programmable phase mask that is insensitive to input polarization.

Note that for the case of fixed linear horizontal or vertical input polarization, this common-mode programming of the retardance is already known to yield a phase-only response. Equation (3), which we report here for the first time to our knowledge, is a significant generalization that shows that this phase-only response applies even in the case of arbitrary input polarization state.

3. Setup

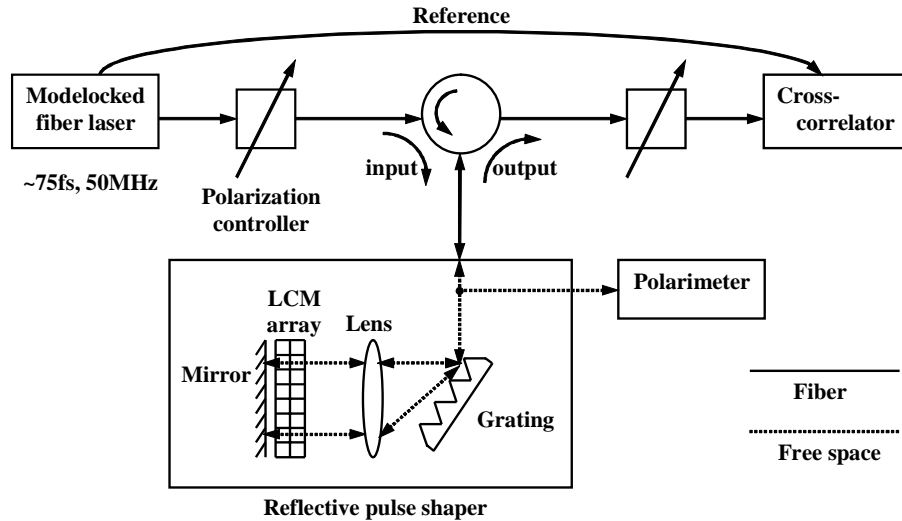


Fig. 1. Complete setup.

Figure 1 shows the schematic for the experiment. A reflection geometry Fourier transform pulse shaper design is chosen because it offers ease of alignment and reduced component count. The reflective shaper receives a 50MHz train of 70-75fs pulses with bandwidth centered at 1575nm from a mode-locked erbium fiber laser [14]. A polarization insensitive fiber circulator separates the incoming pulses from the outgoing waveform. The pulses enter and exit free space via a collimator with output beam diameter of 2.4mm. A low polarization dependent loss (PDL) 600-line/mm diffraction grating at roughly 50° incidence angularly disperses and recombines the beam. The residual PDL of the grating is 0.2-0.25dB per pass; this could be further reduced by using the grating closer to its 34° incident angle design, but at the cost of lower spectral dispersion. A 145mm achromatic lens Fourier transforms the light for conversion to and from spatially separated frequency spots in the mirror plane. A standard two layer, 128-element LCM is programmed in common-mode, as described above, to impart a polarization-independent phase pattern onto the spectrum. Each pixel is 100 μ m wide and 2mm tall; the entire pulse spectrum of 130nm is spread across the 12.8mm aperture with each pixel independently controlling about 1nm of bandwidth. The reflective shaper fiber-to-fiber insertion loss is only 2.9dB (5.1dB including circulator). To our knowledge this is the lowest insertion loss yet reported for a fiber-coupled pulse shaper. Figure 2 shows a photograph of the assembled pulse shaper.

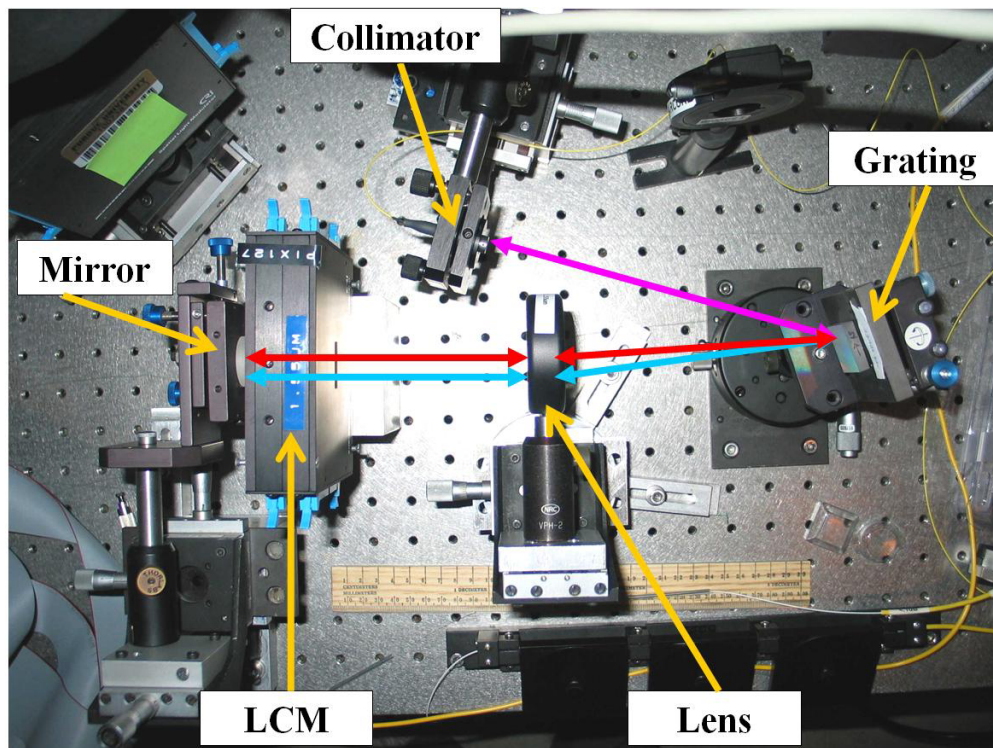


Fig. 2. Photograph of reflective pulse shaper.

4. Experiment

The output pulses are measured via second harmonic generation (SHG) intensity cross-correlation with a reference pulse directly from the laser. Both the reference pulse and the pulse from the pulse shaper are relayed to the cross-correlator using approximately dispersion-

equalized links consisting of matched lengths of standard single-mode fiber and dispersion compensating fiber. The initial measurement shows pulse broadening and distortion, arising from residual cubic spectral phase (dispersion slope) in the fiber link connecting the pulse shaper to the cross-correlator (Fig. 3(a)).

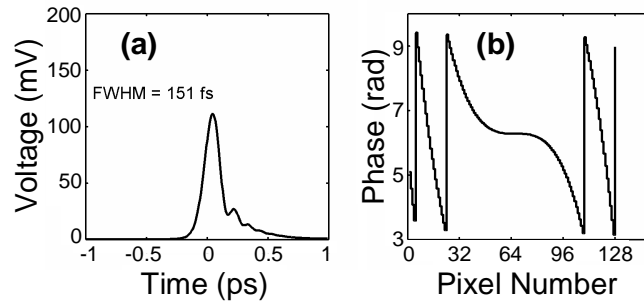


Fig. 3. (a) Uncompensated pulse, note ringing tail. (b) LCM single-pass cubic phase mask.

The LCM is programmed with a compensation mask (Fig. 3(b)) that cancels the cubic spectral phase causing the distortion, resulting in a nearly dispersion free pulse with increased amplitude and a deconvolved pulse width about 75 fs (Fig. 4). Since the LCM array is used in double-pass, the single-pass phase mask plotted in Fig. 3(b) represents half the total spectral phase applied to the pulse. The absolute time position of the pulses is arbitrarily set by the position of the scanning delay stage in our cross-correlation setup and thus the slight shift in the peak pulse position is an artifact of our measurement technique.

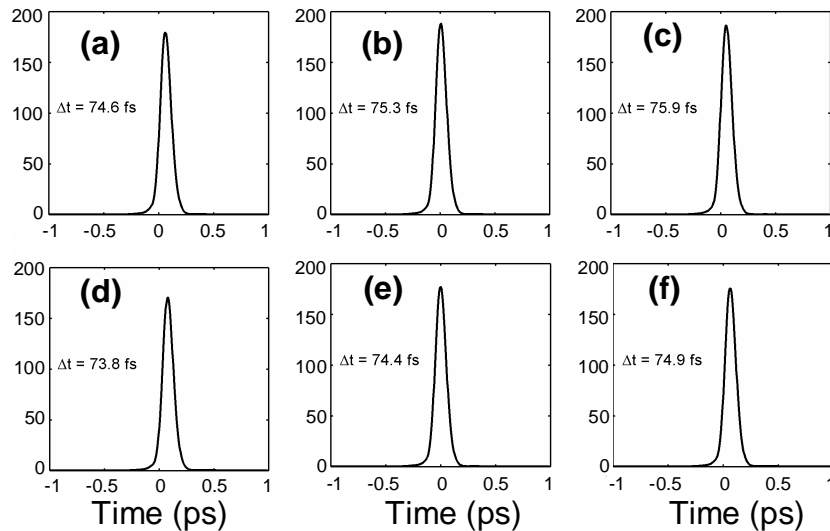


Fig. 4. (a-f) Cross-correlations for the compensated pulse corresponding to the input polarizations given in Table 1. Pulse width is as shown.

As a test for polarization insensitivity, several input polarizations are created, including horizontal, vertical, elliptical states close to right- and left-circular, and two additional elliptical states, as given in Table 1.

Table 1. Six input polarization states

Measured Jones Vector	Approximate Shape
$\begin{bmatrix} 0.76 \\ -0.01 + j0.65 \end{bmatrix}$	Right Circular
$\begin{bmatrix} 0.73 \\ -0.01 - j0.68 \end{bmatrix}$	Left Circular
$\begin{bmatrix} 1.0 \\ 0.0 \end{bmatrix}$	Linear Horizontal
$\begin{bmatrix} 0.0 \\ 1.0 \end{bmatrix}$	Linear Vertical
$\begin{bmatrix} 0.60 \\ -0.75 \pm j0.29 \end{bmatrix}^a$	Elongated Ellipse
$\begin{bmatrix} 0.61 \\ -0.14 - j0.78 \end{bmatrix}$	Rounded Ellipse

^aThe handedness of this polarization was not specifically measured.

The input polarizations are formed by a fiber polarization controller at the input before the circulator and are measured by a free space polarization analyzer (polarimeter) after the collimator. The polarimeter consists of a quarter wave plate and polarizer that are rotated to known angles in order to determine the polarization ellipse. The cross-correlations of the compensated pulses are essentially indistinguishable for all input polarizations tested (Figs. 4(a-f)). In particular, the pulsewidths are identical to within 2 fs, which is within the accuracy limits of our measurement. As a further test, we superimposed onto the compensation mask (Fig. 3(b)) an additional spectral phase pattern, consisting of linear phase ramps with equal but opposite slope in the short and long wavelength halves of the spectrum, respectively (Fig. 5).

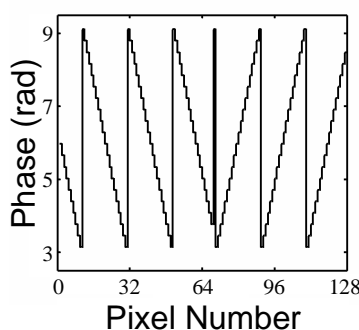


Fig. 5. Doublet phase mask. Spectral slope of $\pm 0.1\pi/\text{pixel}$ for opposite halves of the spectrum.

This results in simultaneous compression and pulse doublet generation. The cross-correlations show a doublet with 1.61 ps spacing, as expected. Again the waveform remains essentially constant for all the input polarizations (Figs. 6(a-f)).

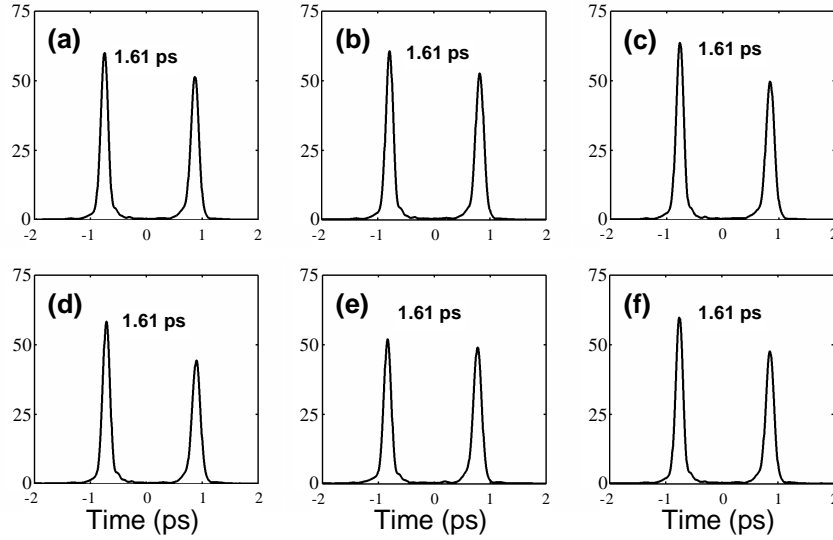


Fig. 6. (a-f) Cross-correlations for a pulse doublet shape corresponding to the input polarizations given in Table 1. Spacing between pulse peaks is as shown.

These results clearly demonstrate spectral phase pulse shaping with functionality that is independent of input polarization.

We also investigated the polarization-dependent loss of our pulse shaping results. Here we note that the intensity cross correlator is itself polarization sensitive due to the tensor properties of the LiIO_3 nonlinear crystal. This measurement issue was addressed by using a fiber polarization controller at the input to the correlator in order to maximize the peak second harmonic signal for each setting of input polarization to the shaper. As evident from the data, output pulses generated from different input polarizations have very similar intensities. To compare the intensities quantitatively, we numerically integrate each of the cross-correlations to find the total power and calculate PDL from the two extreme values according to:

$$PDL_{dB} = 10 \log \left(\frac{P_{Max}}{P_{Min}} \right) \quad (4)$$

For the dispersion compensation experiment, the PDL is 0.44dB; for the experiment corresponding to Fig. 5, the PDL is 0.5 dB. These PDLs are fully consistent with the residual PDL of the grating and are much lower than numbers that have previously been reported for polarization pulse shaping [11,13]. Furthermore, our results provide evidence that the state of polarization remains independent of frequency throughout the pulse shaping process; otherwise the polarization selective nature of the SHG process would lead to strong, input-polarization-dependent variations in the cross-correlation intensities, which are not observed.

5. Conclusion

In summary, our results clearly demonstrate polarization-independent spectral phase pulse shaping, with low loss and low PDL. This work should facilitate practical applications in fiber optics, where polarization insensitivity is an important requirement.

Acknowledgements

This work was funded in part by the National Science Foundation under grant 1040682-ECS and by the Cisco University Research Program.